Journal of Hydrology 570 (2019) 637–646

Contents lists available at ScienceDirect

Journal of Hydrology

journal homepage: www.elsevier.com/locate/jhydrol

Research papers

Optimizing the riparian zone width near a river for controlling lateral migration of irrigation water and solutes

V. Phogat[a,b,*], J.W. Cox[a,c], Rai S. Kookana[d], J. Šimůnek[e], T. Pitt[a], N. Fleming[a]

[a] South Australian Research and Development Institute, GPO Box 397, Adelaide, SA 5001, Australia
[b] CCS Haryana Agricultural University, Hisar 125 004, India
[c] The University of Adelaide, PMB1, Glen Osmond, SA 5064, Australia
[d] CSIRO Land and Water, PMB No. 2, Glen Osmond, SA 5064, Australia
[e] Department of Environmental Sciences, University of California, Riverside, CA 92521, United States

ARTICLE INFO

This manuscript was handled by Peter K. Kitanidis, Editor-in-Chief, with the assistance of Karl Vanderlinden, Associate Editor

Keywords:
Buffer width
Irrigated crops
HYDRUS
Leaching
Solute dynamics
Water quality

ABSTRACT

Riparian zones are essential to preserve water quality of rivers adjacent to large areas of irrigated agriculture. We used HYDRUS (2D/3D) to quantify the long-term (8 years) influence of crops (almonds, wine grapes and potato-carrot) irrigated with recycled water on water and solute exchange at the Gawler River interface in relation to vegetation buffer widths from 10 to 110 m. We found that under almond and annual horticulture the likely average annual water flow from the irrigated area to the river was nearly twice as much (2.1 and 1.8, respectively) that under wine grapes. The hydraulic exchange at river interface for different irrigated crops was found to be sensitive to the buffer widths. For wine grapes, almonds and annual horticulture, the average annual hydraulic balance reached an equilibrium at 20, 65 and 55 m buffer widths, respectively. Furthermore, for wine grapes, with a 20 m buffer width, the average annual load of salts became negligible. This study shows that buffer widths of 20, 60, and 40 m for irrigated wine grapes, almond, and annual horticulture, respectively, are needed to restrict the migration of salts to the river. Further refinements are possible by incorporating the influence of preferential flow paths, improved water stress response functions, and addressing the data limitations for calibration of the model for solute dynamics.

1. Introduction

Crop production, especially in arid and semi-arid regions of the world where rainfall is not able to meet the evapotranspiration needs of the crops, depends on supplemental irrigation. Irrigated agriculture contributes 40% of the world food production from 20% of the cropped area, thus makes a major contribution to the global food security (FAO, 2016). However, irrigated agriculture may become unsustainable due to its contribution to soil degradation, salinization, waterlogging, and environmental pollution. Global water security warrants beneficial reuse of recycled water, such as irrigation, but with minimal potential harmful impacts on ecosystems. Ecosystem impairment, particularly reduced soil quality, biodiversity loss, and harm to amenity and cultural heritage values, is a growing global problem (FAO, 2011). Therefore, future irrigation schemes must address trade-offs, particularly with respect to inter-sectoral water allocations and environmental impacts.

Aquatic ecosystems adjacent to irrigated agriculture are most at risk due to the transport of irrigation induced chemicals such as soluble salts, nitrates, and pesticides (Zhang et al., 2010). The fate of these chemicals in the soils and their migration to receiving environments depend on a number of factors including the vegetation, topography, climate, soil, irrigation, groundwater level, and flow conditions in the stream (Klatt et al., 2017; Schilling et al., 2018). Riparian vegetation can moderate the movement of water and solutes to water bodies by interception and attenuation of chemicals moving through the buffer zone (King et al., 2016).

Several investigations have examined the functions of buffer zones for stream ecosystems (e.g., Mayer et al., 2007; Hansen et al., 2010). However, these have mostly dealt with the overland movement of solutes via surface runoff and sediment transport. Only, a limited number of modelling or case studies have evaluated the role played by buffer zones in reducing the migration of irrigation induced soluble salts/contaminants via subsurface flow to streams (e.g., Naiman et al., 2005; Allaire et al., 2015). Subsurface flow paths can exhibit wide variations depending on specific local conditions (Naiman et al., 2005) including subsurface lithology and stratigraphy (DeVito et al., 2000; Hill et al.,

* Corresponding author at: South Australian Research and Development Institute, GPO Box 397, Adelaide, SA 5001, Australia.
E-mail address: vinod.phogat@sa.gov.au (V. Phogat).

https://doi.org/10.1016/j.jhydrol.2019.01.026
Received 24 July 2018; Received in revised form 13 January 2019; Accepted 21 January 2019
Available online 25 January 2019

2004). To our knowledge, no information is currently available in the literature on the role played by buffer zones in dealing with the irrigation induced solute interception or influencing its migration to water bodies.

Field experiments for assessing the role of a buffer zone on the subsurface water and salts movement from irrigated cropping system to an adjoining river is both a complex and expensive exercise. Therefore, numerical models are increasingly being used (e.g., Flipo et al., 2014; Xian et al., 2017) for such assessment. Hydraulic exchange across the stream-aquifer has been modelled with buffer zones (e.g., Phogat et al., 2017a) or without (e.g., Baratelli et al., 2016). Similarly, Kidmose et al. (2010) employed a conceptual groundwater flow and reactive transfer model to establish a relationship between flow paths and the fate of a pesticide in a riparian wetland. Alaghmand et al. (2013) used a numerical model (Hydrogeosphere) to evaluate the interaction between a river and a saline floodplain in relation to groundwater fluctuations, incorporating evapotranspiration losses by riparian vegetation. Klatt et al. (2017) explored the capability of a coupled hydro-biogeochemical model to evaluate the effectiveness of buffer strips to reduce nitrogen loads into aquatic systems. However, most of these modelling studies have been either conceptual and/or only partially calibrated for site-specific flow and/or solute dynamics. The complicated nature of water and solute transport processes (Sophocleous, 2010) and the inherent uncertainty of input data are some of the challenges in simulating water flow and solute transport with physically based models. Nevertheless, such models are valuable in understanding water flow and solute transport/reaction processes involved in complex bio-geological environments.

This study uses a two-dimensional finite element numerical model HYDRUS (2D/3D (referred to below as HYDRUS; Šimůnek et al., 2016) to quantify the extent of water and solute exchange across a stream-buffer interface. The study involves complex heterogeneous geological formations involving real-time climatic, vegetative (crop and buffer), and stream flow conditions. The key objectives of this investigation were: i) to calibrate and validate a numerical model (HYDRUS) for water table dynamics in an area adjacent to a seasonal river (Gawler River) by incorporating daily water level fluctuations in the river, groundwater dynamics, crop evapotranspiration, riparian zone vegetation evapotranspiration, and soil heterogeneities; ii) to estimate the impact of different buffer zone widths on the flux exchange at the river-buffer interface under different cropping systems, iii) to optimize the riparian width to control the irrigation-induced solute movement to the river for different irrigated crops; and iv) to estimate the residence time of the solute tracer migrating to the adjoining water body through the subsurface under shallow water table conditions.

2. Materials and methods

2.1. Experimental site

The study was carried out at the Virginia Park (34°38′2.6″S and 138°32′27.6″E) gauging station at Gawler River which is situated at 12 m above the Australian Height Datum (AHD). The Gawler River only flows during the rainy season (July to October). However, stagnant water (about 30–100 cm)/base flow conditions prevail at other times at the gauging station. The adjacent area, being a part of the vast Northern Adelaide Plains (NAP), has a relatively flat topography with a gentle slope to the west. All relevant features of the study site are shown in Fig. 1. The NAP experiences a Mediterranean climate, which is characterised by hot, dry summers and cool to cold winters. Long-term (1900–2016) average rainfall in the region amounts to 475 mm (Department of Environment, Water and Natural Resources, 2016) and annual evapotranspiration amounts to 1308 mm, resulting in the irrigation demand for crop production. Water table fluctuations in the area adjacent to the river were monitored in the shallow wells (PTA100, PTA101, PTG078, and PTG080). Location of these wells is shown in Fig. 1.

2.2. Soil characteristics

The soils of the NAP are highly heterogeneous with depth. There is commonly a shallow clay layer at a variable depth, which determines the root growth and crops to be grown. Broader soil groups and geology of the site were obtained from the stratigraphic information of the site and well logs within the vicinity of the site. There are in general 6 major geological layers, which include red friable sandy loam soil, light brown silty topsoil, sandy clay, sandy non-calcareous clay, non-calcareous fine sandy clay, and sand. The soil particle size distributions and bulk densities of these soil groups were obtained from the previous soil analysis reported in ASRIS (ASRIS, 2011) and the APSIM (Holzworth et al., 2014) data base. The particle size and bulk density data were used to estimate soil hydraulic parameters using the ROSETTA module embedded in the HYDRUS software environment. The saturated hydraulic conductivity (K_s), and the α and n parameters were further adjusted during the calibration process and their final optimized values are presented in Table 1.

2.3. Buffer and crops parameters

The vegetation buffer at the study site is dominated by river red gums (*Eucalyptus* spp.) but its width is highly variable along the longitudinal distance of the river, ranging from a couple to hundreds of metres. The area adjoining the riparian buffer is used for intensive cropping such as almonds, wine grapes, potato, carrot, and onion all along the river. On the southern side of the river where the modelling domain was established, the land has been used for the wine grape cultivation.

Daily crop evapotranspiration (ET_C) for river red gum (*Eucalyptus* spp.) in the buffer zone and irrigated crops (wine grape, almond, carrot, potato) grown in the adjacent river corridor were estimated from daily reference crop evapotranspiration (ET_0) data and local crop coefficients (K_c). The ET_O (Allen et al., 1998) data was obtained from the nearby weather station (Edinburg Raaf). The daily ET_C values were divided into evaporation (E_s) and transpiration (T_p) components based on the leaf area index (LAI) as follows (Ritchie, 1972):

$$E_s = ET_c \cdot e^{-K_{gr} \times LAI} \quad (1)$$

$$T_p = ET_c - E_s$$

Here, K_{gr} is the light extinction coefficient for global solar radiation and its value was set to 0.5 (Aubin et al., 2000; Phogat et al., 2017a) for all vegetations. The LAI data for wine grapes and almonds was obtained from other studies (Phogat et al., 2017b, 2018b) and for the annual horticulture (carrot and potato) crops from the literature (Reid and English, 2000; Deshi et al., 2015). Canopy interception by the buffer vegetation was assumed to be 15% of precipitation (Xiao et al., 2000). Estimated daily E_s and T_p values and daily rainfall were used as input in HYDRUS simulations.

The roots of the buffer strip vegetation were assumed to be distributed linearly from the soil surface to a depth of 200 cm. Although roots of *Eucalyptus* can grow to a depth of 6–7 m (Phogat et al., 2017a), however, due to shallow water table conditions at the site, roots generally did not grow far below a water table due to the lack of the oxygen supply (Baker et al., 2001). Similarly, the rooting depths of 100, 200, and 60 cm for wine grape, almond, and annual horticulture (carrot and potato), respectively, were used in the modelling study based on relevant studies from the region (Phogat et al., 2017b, 2018b). The root water uptake parameters for almond and wine grape were also taken from these studies and the HYDRUS database (potato and carrot). Since HYDRUS does not allow using different parameters for stress response functions for the crop and buffer zones, hence the same Feddes' parameters (Feddes et al., 1978) were used for both parts of the domain. It

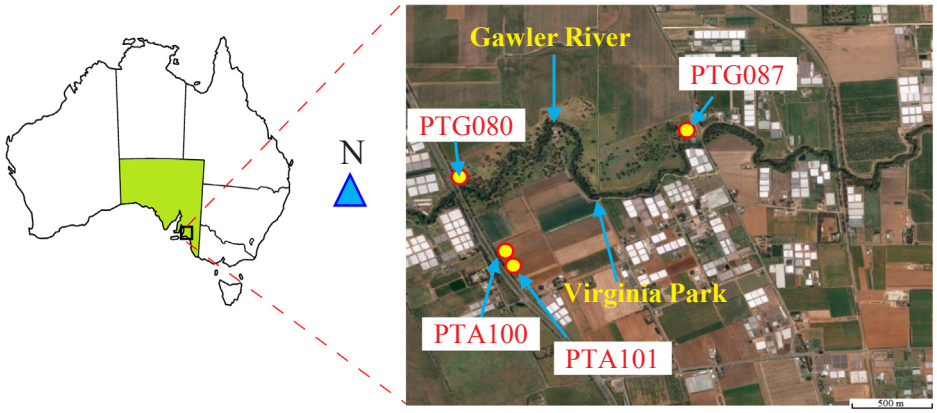

Fig. 1. Map of the study site showing the Gawler River, the gauging station, shallow wells (yellow circles) and adjacent cropped area. (For interpretation of the references to colour in this figure legend, the reader is referred to the web version of this article.)

Table 1
Optimized soil hydraulic parameters used in numerical simulations.

Sr No	Textural class	Depth (m)	θ_r (cm^3cm^{-3})	θ_s (cm^3cm^{-3})	α (cm^{-1})	n	K_s ($cm\ d^{-1}$)	l
1	Sandy loam	0–1	0.07	0.44	0.024	1.45	56.1	0.5
2	Silty loam	1–2	0.06	0.45	0.03	1.5	69.8	0.5
3	Clay loam	2–5.5	0.07	0.43	0.0227	1.414	39.9	0.5
4	Silty clay loam	3.5–6	0.08	0.44	0.023	1.303	25.0	0.5
5	Sandy clay	6–8	0.09	0.44	0.0234	1.268	18.8	0.5
6	Sand	8–12	0.05	0.41	0.124	2.28	350.	0.5

must be noted that root water uptake in HYDRUS depends on the availability of water in the soil, the root spatial distribution, and differential transpiration fluxes in the crop and buffer zones. The root water uptake was assumed to be linearly distributed with depth, with the maximum at the soil surface and zero at the bottom of the rooting zone.

The "trigger irrigation" option was used to generate irrigation schedules for all crops (wine grape, almond, annual horticulture). The trigger pressure used for wine grapes, almond, and carrot-potato, respectively, were −60, −25, and −15 kPa at a depth of 30 cm. Similar trigger pressures have been used for these crops in previous studies (Green, 2010; Phogat et al., 2018a,b).

2.4. Transport domain, initial and boundary conditions

The transport domain represents a 400 m cross section from the middle of the river (Fig. 2). The vertical dimension represents the distance from the Australian Height Datum (AHD) to the soil surface (12 m) at the experimental site. The top width of the river was 10 m, the bottom width 4 m, and the depth 4 m at the study site. The width of the buffer zone is 30 m from the river bank. Therefore, the lateral width of the riparian zone at the Virginia Park gauging station from the middle of the river is approximately 35 m, which also includes an unsealed road which runs along the river. The finite element discretization resulted in 10,000 2D elements in a standard rectangular 2D domain.

On the upper left side of the domain (Fig. 2), the atmospheric boundary was considered through which the infiltrative influx or the evapotranspirative efflux occurs. A time-variable flux boundary condition (treated similarly as an atmospheric boundary condition) was imposed on the upper right side of the domain to represent the buffer zone, which had different fluxes than the irrigated surface. The flux at this boundary was given by the difference between daily rainfall and daily potential evaporation (E_s). A special HYDRUS boundary condition (BC) was specified in the river. This special BC assigns the hydrostatic pressure head on the boundary below the water level in the river and a seepage face BC on the boundary above the water level. The specified water levels in the river are linearly interpolated in time in order to smooth the impact of daily fluctuations of water levels in the river (Phogat et al., 2017a). Measured values of water table depths in the well near the left boundary of the domain (PTA100) were used to define initial and time-variable pressure head boundary conditions. No flow was assumed as the boundary. The initial pressure head condition in the domain was specified by interpolating measured mean water table depths in the shallow wells (Fig. 1) in the adjacent area while considering hydrostatic equilibrium conditions in the vertical direction. Daily rainfall in excess of the soil infiltration capacity is accounted for as run off by HYDRUS. The longitudinal dispersivity was assumed as one tenth of the modeling domain (with the transverse dispersivity

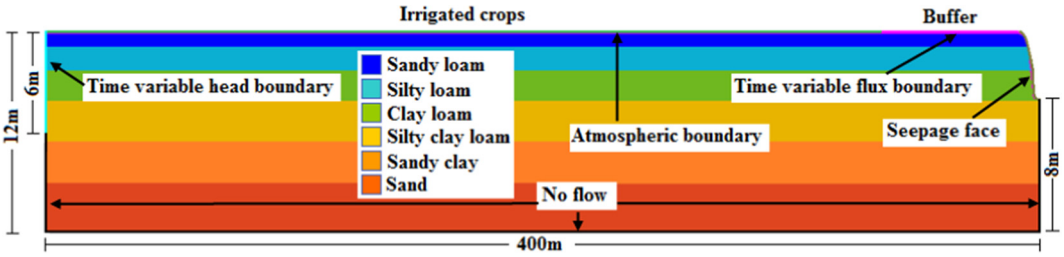

Fig. 2. Schematic representation of the flow domain showing the material distribution, the river, the buffer strip, irrigated crops, and imposed boundary conditions.

being one tenth of the longitudinal dispersivity) (Cote et al. 2003; Phogat et al., 2014) and the molecular diffusion coefficient in water equal to 1.66 cm^2/day (Phogat et al., 2018b).

2.5. Calibration and validation of the model

Measured water table depths (average of four quarterly measurements in a year) in the shallow wells (PTA101, PTG080 and PTG087, Fig. 1) near the study site were used for the calibration and validation of the model. Simulations were carried out for 1461 days (1st July 2009 to 30th June 2013) to calibrate the model for water table depths at the middle of the domain (X = 200 m). For most sensitive model parameters including the saturated hydraulic conductivity (K_s), and the coefficients α and n of different soil layers were varied manually and no automated parameter optimization procedure was used to calibrate the model. In addition to a visual comparison of observed and simulated water table depths, a quantitative evaluation of the model performance was undertaken using goodness-of-fit measures (see Section 2.7) similar to other studies (e.g., Alaghmand et al., 2013, 2014). The calibrated model was validated for 1461 days (1st July 2013 to 30th June 2017) by comparing the measured and simulated water table depths. The calibrated and validated model was then used to assess the impact of other irrigated crops (almond and annual horticulture crops such as carrot and potato) and the buffer zone widths on the migration of water and solutes to the river. More details on different scenarios are given below in the Scenario Analysis section.

To understand the movement of irrigation-induced solutes/agrochemical tracers to the river water, we considered Total Dissolved Solids (TDS) as representative of all soluble solutes which is consistent with numerous studies (e.g., Ramos et al., 2011; Phogat et al., 2014, 2018b). The initial soil conditions in the domain were assumed to be solute free. The average quantity of TDS (1200 mg/L) of Class-A treated (recycled) water from the Bolivar treatment plant (Stevens et al., 2003) was applied during all triggered irrigations at the atmospheric boundary where crop is being grown. However, the model calibration for solute dynamics could not be conducted due to the non-availability of site-specific data for solute transport processes.

2.6. Scenario analysis

The calibrated and validated model was then used to simulate the dynamics of the hydrological fluxes and solute movement for different buffer widths and for various irrigated crops (wine grape, almond, and carrot-potato rotation). The simulations were executed for 8 years (1st July 2009 to 30th June 2017) plus further 8 years if needed (if solute did not reach the river) for all 3 irrigated crops for varying buffer zone widths (10–110 m) from the centre of the river. These simulations were established to evaluate the appropriate width of the riparian zone to control the lateral movement of solutes to the river. In the simulations extended in future climate (8 years), median climate change data for the Edinburg RAAF station were used (Charles and Fu, 2015). Initial conditions and daily water level fluctuations for such future simulations were imported from the previous simulations (8 years). To estimate the extent of leaching, the annual water balance for different crops was computed using inputs such as rainfall, irrigation, and model-simulated evaporation and transpiration and assuming similar initial pumping well and river exchange conditions in the domain.

2.7. Model evaluation

The model's performance was evaluated by comparing measured (M) and HYDRUS simulated (S) water table depths. Correlation coefficients were estimated to understand the relationship between measured and simulated values of water table depths during the calibration and validation periods. The statistical error estimates [mean error (*ME*), mean absolute error (*MAE*), and root mean square error (*RMSE*)] between the measured and simulated water table depths were estimated as:

$$ME = \frac{1}{N}\sum_{i=1}^{N}(M_i - S_i) \tag{2}$$

$$MAE = \frac{1}{N}\sum_{i=1}^{N}|M_i - S_i| \tag{3}$$

$$RMSE = \sqrt{\frac{1}{N}\sum_{i=1}^{N}(M_i - S_i)^2} \tag{4}$$

Many studies (e.g., Coffey et al., 2004; Alaghmand et al., 2013) have used similar goodness of fit measures (correlation coefficients and RMSE) as above.

We also evaluated the test of significance between the measured and simulated values of water table depths using the paired t-test (t_{cal}) as below:

$$t_{cal} = \frac{d}{SD_m\sqrt{\frac{1}{n}}} d = \bar{M} - \bar{S} \quad \text{and} \quad SD_m = \sqrt{\frac{ns_1^2 + ns_2^2}{2n-2}} \tag{5}$$

Here, n is the number of comparable paired points, s_1 and s_2 are the standard deviations of measured and simulated data, respectively, d is the different between measured ($\bar{M}$) and simulated ($\bar{S}$) means values, SD_m is the standard deviation of the mean, and t_{cal} is the calculated paired t-test value. The null hypothesis tests that there is no significant difference between the mean values of measured and simulated water table depths.

Nash and Sutcliffe (1970) model efficiency (E) is a normalized statistic that expresses the relative magnitude of the residual variance compared to the variance of the measured data during the period under investigation, as given below:

$$E = 1 - \frac{\sum_{i=1}^{N}(M_i - S_i)^2}{\sum_{i=1}^{N}(M_i - \bar{M})^2} \tag{6}$$

The range of E lies between $-\infty$ and 1.0 (a perfect fit). An efficiency value between 0 and 1 is generally viewed as an acceptable level of performance. Efficiency < 0 indicates that the mean value of the observed time series would be a better predictor than the model and denotes unacceptable performance (Moriasi et al., 2007; Legates and McCabe, 1999).

3. Results and discussion

3.1. Calibration and validation of HYDRUS-2D

The data in Fig. 3 demonstrates a consistent performance of the model (i.e. R^2 of 0.66 and 0.64, and E = 0.34 and 0.34, respectively) during calibration (2009–2013) and validation (2013–2017) period. These values fell within the R^2 values (0.35–0.84) reported in other modelling studies (e.g., Coffey et al., 2004; Phogat et al., 2016). Other statistical estimates (*ME*, *MAE*, *RMSE* and *SD*; see Fig. 3) during the calibration and validation period were similar but slightly higher than previously observed values (e.g. Alaghmand et al., 2013). This is because of wide fluctuation within the input data. The paired t-test indicated that there was no significant difference (p = 0.05) between the measured and simulated mean depths of water table. Overall, all these statistics confirm an adequate representation of groundwater fluctuations by the model.

Calibration of the model for solute dynamics was not possible due to the lack of site specific data. However, numerous studies have shown that sufficiently calibrated and validated model for complex hydraulic fluxes in a heterogeneous domain can offer valuable practical understanding of bio-geochemical processes in the soil. For example,

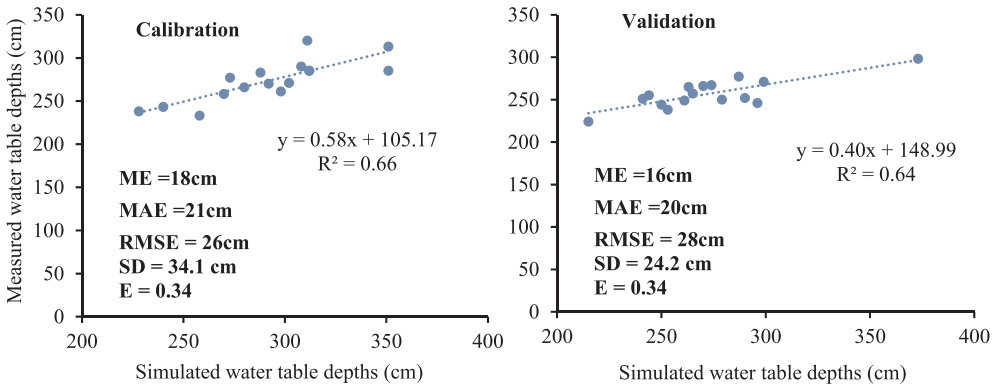

Fig. 3. Relationship between measured and simulated water table depths, statistical error estimates (ME, MAE and RMSE), standard deviation (SD) and model efficiency (E) values during the calibration (2009–13) and validation (2013–17) periods.

Alaghmand et al. (2013, 2014) indicated that the complexity associated with the quantification of the solute transport parameters restricted them from validating the model on the observed concentration pattern. However, their study unravelled the impacts of groundwater pumping on salinization risks of a flood plain. Similarly, Carr et al. (2018) calibrated and validated a 2D model on gauged groundwater elevations and hypothesized that the accurate representation of flow dynamics can inform environmental management involving transport of sediments, nutrients, and heavy metals. Other studies also have used similar approaches (e.g., Rousseau et al., 2012).

3.2. Irrigation and annual water balance for crops

The extent of average annual irrigation among all crops during 2009–2017 (Fig. 4) was the lowest in wine grape (242 and 320 mm), followed by almond (760 and 920 mm) and the highest for annual horticulture (951 and 1226 mm) reflecting their specific evapotranspiration requirements (Phogat et al., 2018b). Correspondingly, the leaching fraction/recharge flux under almond (87–298 mm) and annual horticulture (100–252 mm) was 3–3.8 times higher than under wine grapes. Besides for wine grapes, a negative annual flux balance was recorded in some years but, the overall average balance was positive over 8 years. These observations are consistent with other studies (Green, 2010; Reynolds, 2010; Phogat et al., 2018b). It is well understood that the contribution of leaching fraction/irrigation return flow from irrigated crops can be a critical driver for the river-buffer hydraulic exchange (e.g., Berens et al., 2009).

3.3. Hydraulic exchange at the river-buffer interface

Numerous high rainfall/flood events during 2009–2017 resulted in large amounts of recharge as indicated by large peaks in Fig. 5. During summer, a large amount of irrigation is applied to crops in the adjoining area, which reverses the flow gradient across the buffer-river boundary. Under such dynamic conditions, aquifer recharge or discharge may occur depending on the river level (Ghazavi et al., 2012), leading to either a gaining or losing river (Rassam, 2011; Phogat et al., 2017a). However, irrigation-induced flow to the river depends on the water uptake/evapotranspiration pattern of buffer zone vegetation (Phogat et al., 2017a) and on the extent of return flow from the irrigated areas. As shown earlier, the extent of irrigation-induced flow (recharge) is higher for almond and annual horticulture as compared to wine grapes (Fig. 4). As a result, the average annual amount of flux exchange at the river interface was nearly twice (1.8–2.1 times) as much under almond and annual horticulture than under wine grapes (Fig. 5). Additionally, the high evaporation demand of the buffer zone vegetation may further limit the net discharges to the river. This was probably not met by the low drainage flux under wine grapes. Overall, irrigation induced drainage, groundwater discharge to the stream, evapotranspiration by the buffer zone vegetation and irrigated crops play a key role in defining the extent of exchange between the buffer zone and the river.

The impact of different buffer widths on the average annual water exchange at the river interface for different irrigated crops is shown in Fig. 6. For wine grapes, the average annual hydraulic balance was negative for the 10–20 m buffers during the simulation period (8 years, 2009–2017), indicating the dominance of flow from the irrigated area to the river system. However, the reverse was observed for buffer widths > 20 m as the evapotranspiration demand of the buffer vegetation governed the water exchange at the river-buffer interface. In the case of almond, however, the overall water balance remained negative (discharge to the river) for a buffer zone up to 65 m due to its 3 times higher irrigation than for wine grapes. Similarly, under annual

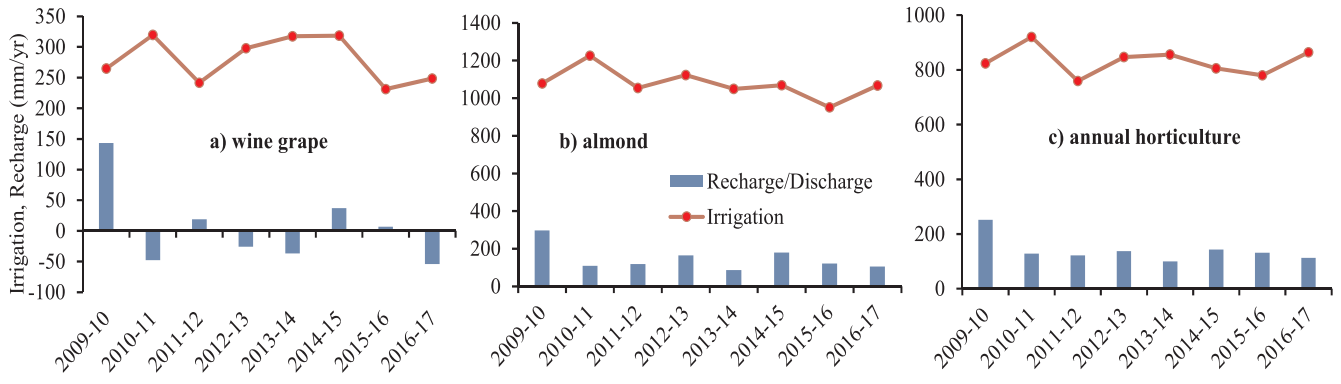

Fig. 4. Annual irrigation (mm) and recharge/discharge (mm) in the domain under a) wine grape, b) almond, and 3) annual horticulture (carrot-potato) crops. Positive fluxes are recharge and negative fluxes are discharge from the domain.

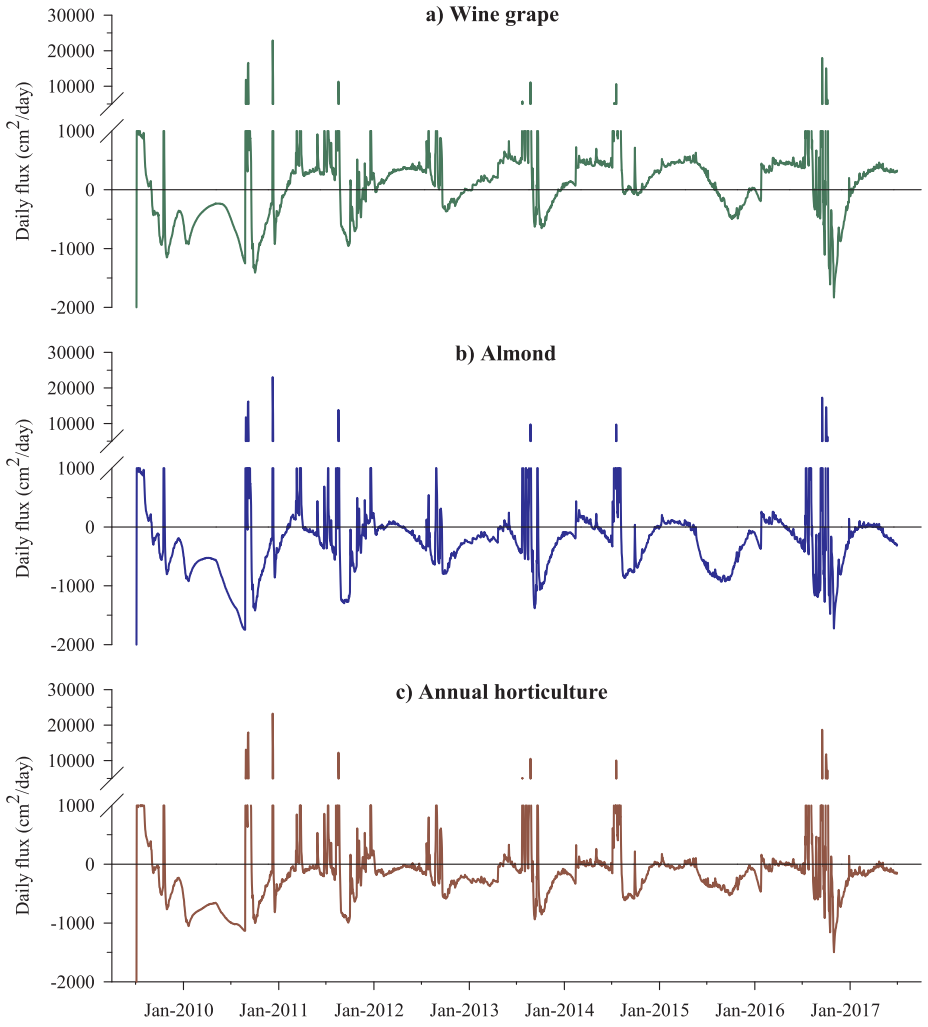

Fig. 5. Daily flux exchange at the river-buffer interface for almond, wine grape, and annual horticulture (carrot-potato) grown near the Gawler River during 2009–2017.

horticulture (carrot and potato) crops, the overall hydraulic balance was similar to almonds and the threshold buffer zone width for equilibrium flow conditions reached at 55 m (Fig. 6). Based on irrigation regime for irrigated crops, different buffer zone widths are required for equilibrium flow conditions at the river-buffer interface.

3.4. Impact of a buffer width on solute dynamics

Temporal dynamics of irrigation induced salts in the soil profiles with 30 m buffer widths for wine grapes, almonds, and annual horticulture is shown in Fig. 7. Irrigation induced salts gradually moved downwards as well as laterally, but, the vertical movement was faster. Initially, salts continued to build up in the soil and then migrated to the shallow groundwater (water table at 4 m). It was noted that the irrigation induced salts entered the shallow groundwater within 2 years of irrigation of almond and annual horticulture (Fig. 7), but it took longer for wine grapes. It is noteworthy that after 8 years of simulation, the salts were distributed in variable concentrations throughout the entire

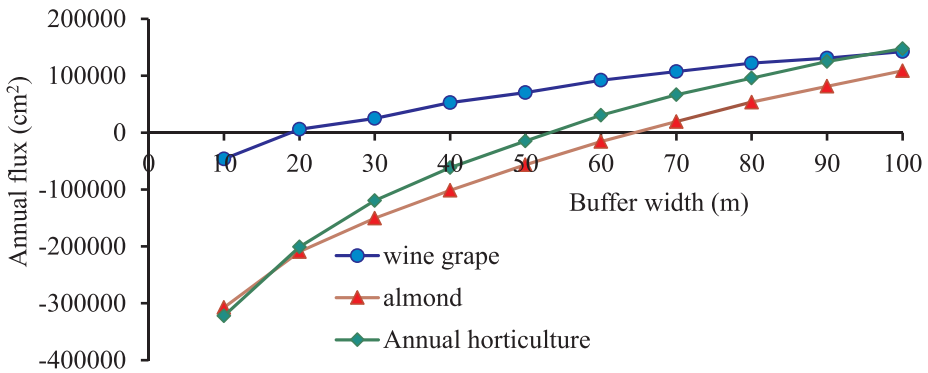

Fig. 6. An average balance of water exchange across the stream-aquifer interface for different buffer widths under a) wine grapes, b) almond, and c) annual horticultural crops.

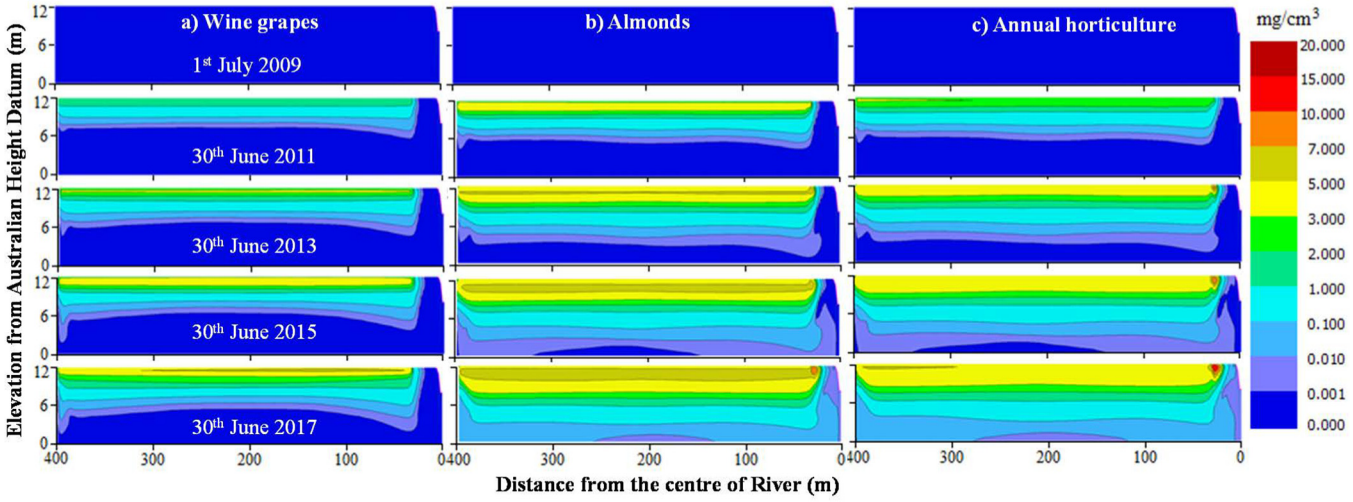

Fig. 7. Temporal dynamics of irrigation induced salts in the soil profile with a 30-m buffer width under a) wine grapes, b) almonds, and c) annual horticulture (carrot-potato) at the indicated times during 2009–2017. The river is situated at the top right corner of the domain.

domain, including along the river boundary, especially for almond and annual horticulture. The presence of salts along the river boundary indicates that they may have already entered into the river system in low concentrations (< 0.0011 mg/cm^3) against the concentration gradient under these crops. In contrast, for wine grapes, salts travelled a far shorter distance than for the other two crops and the salt plume remained far from the river front boundary (Fig. 7). Nonetheless, the extent and timing of salts migration into the river system was not clearly visible.

Excessive concentrations of soluble salts as shown on the right hand corner of Fig. 7 for almond and annual horticulture can have an adverse impact on plant growth and transpiration losses. However, this situation was obtained for a 30 m buffer width (Fig. 8), which is an insufficient width to control salts mobilization to the river for these crops. This shows that in the absence of an adequate buffer width, there is a chance of rapid secondary salinization close to the river. In such situations, adopting native vegetation such as river red gums (with a salt tolerance of 30 dS m^{-1}) or black box trees (salt tolerance of 55 dS m^{-1}) as buffer (Overton and Jolly, 2004), could help maintain appropriate transpiration services in such situations (Alaghmand et al., 2013, 2014).

The frequency, timing, and load of salt pulses entering into the river during 8 years (2009–2017) of simulation under different crops as influenced by buffer zone widths is shown in Fig. 8. It is apparent that for wine grapes, the salts/tracer pulse appeared in the river only for buffer widths < 20 m. Further widening the buffer (30–60 m) and extending the simulations to 16 years (2009–2025; data not shown) did not produce any appreciable amount of salts in the river. In contrast, a significant salts/tracer pulse continued to appear in the river for 50 and 60 m buffer for annual horticulture and almond irrigated crops, respectively, during 8 years (2009–2017) of simulation. Further extending the buffer (up to 100 and 110 m) and simulation time (2009–2025) resulted in a very small amount of tracer salt to appear in the river (10^{-22} to 10^{-6} mg) for annual horticulture and almond. Therefore, it is concluded that a buffer width of 20, 50 and 60 m for wine grapes, annual horticulture (carrot-potato) and almonds, respectively, is needed to restrict the subsurface migration of irrigation induced salts/tracer chemicals to the river.

In terms of salt load the same buffer width for different crops released varying pulses in the river (Fig. 8). For example, for a buffer width of 10 m for almond during the 8 years of simulation was approximately twice the salts load than that for annual horticulture, which in turn had 10 times higher loads than wine grapes. However, with increasing buffer width (e.g. 20 m), salts loads were drastically decreased (especially in almonds and annual horticulture), but, the timing of occurrences of salts/tracer pulses in the river are similar irrespective of irrigated crops. Notably, a large solute peak occurred in the river water after approximately 7 years of simulations (August to December 2016), which transported different amounts of salt to the river at different buffer widths. This time corresponds to the aftermath of a flood event when the water level in the Gawler River reached the soil surface and completely saturated the adjacent riparian zone. Subsequent receding water levels in the river created a steep gradient from the buffer zone to the river, which conveyed a large amount of salts from the saturated zone to the stream. Such observations were also reported in other studies (Bryan et al., 1998; McKergow et al., 2003). Hence, the salts transported to the river may not be associated only with irrigation, but also with the generation of hydraulic gradients, which push the salts laterally into the river. However, the impact of hydraulic gradients gradually dissipates as the buffer width increases, since the buffer zone acts as a barrier in transmitting the hydraulic response between the river and the irrigated area. Overall, it appears that all components of soil, water, crop and climate, play a crucial role and have a different influence on the salt transport to the river and its water quality.

Salts load transported to the river and the residence time of solutes in the soil for different buffer widths and crops are shown in Fig. 9. The amount of salts for the 10 m buffer was very similar for almond and annual horticulture and about 40 times higher than for wine grapes. Meanwhile, the salts transported to the river for the 20 m buffer were higher for annual horticulture than for almond. When the buffer width was increased to 60 m, only a small additional reduction in the salt load was observed (99.9%). Similarly, for annual horticulture, the average annual load of salts was reduced by 92.2% (to 1566 mg) for the 20 m buffer width as compared to the 10 m buffer width. For a 99.9% reduction in the salt load, a 40 m buffer width is needed. Therefore, it is established that maintaining a 20, 60, and 40 m buffer widths for wine grapes, almonds, and annual horticulture can effectively reduce irrigation induced salts/tracers transport to the river by 99.9%.

The residence time was twice as long for wine grapes as compared to almonds and annual horticulture for buffers < 40 m wide. For example, the residence time for a 10 m buffer was 2.5 months for almonds and annual horticulture, and 5 months for wine grapes (Fig. 9). The residence time for the solute movement to the stream starts increasing exponentially for larger buffer widths (> 40 m) and wine grapes. It took about 7 years for irrigation induced solutes, though concentrations were very small, to appear in the stream when the buffer width was 60 m. The residence time for almonds and annual horticulture was very

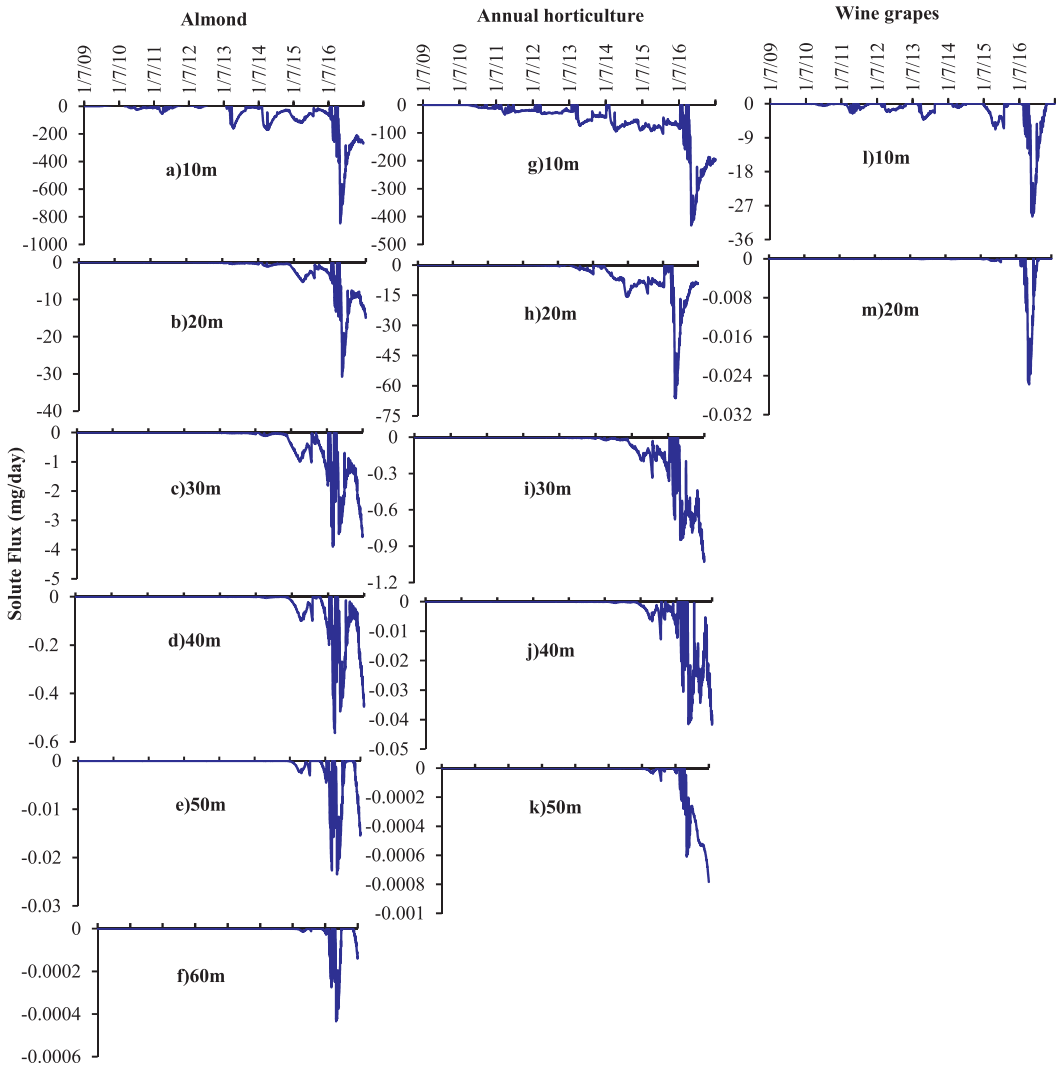

Fig. 8. The effect of buffer zone widths (10, 20, 30, 40, 50 and 60 m) on the lateral migration of irrigation induced salts into the river under almond (a to f), annual horticulture (g to k), and wine grapes (l to m) during 2009–2017. The solute flux scale at the vertical axes is different in different figures.

small (< 100 days) for buffer widths < 30 m, then gradually increased to 450 days for a 70 m, and to much longer values for larger buffer widths. A longer residence time for wine grapes is associated with a relatively low recharge volume, which was unable to generate a sufficient hydraulic gradient to push the salts into the river. Therefore, the extent of irrigation return flow is crucial for the longevity of solutes in the soil system. The knowledge of the time required for the migration of salts to the river helps in devising guidelines for maintaining the river

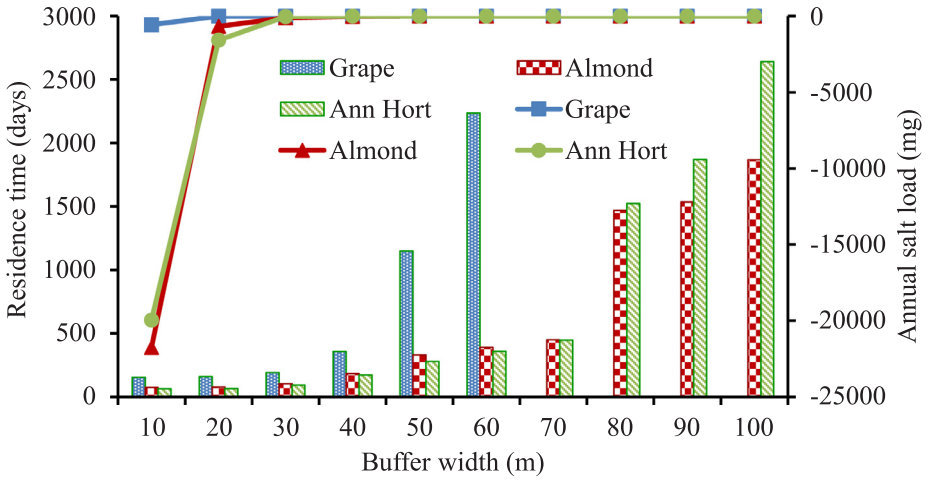

Fig. 9. The amount of salts (line graph) and their residence times (bars) for different irrigated crops as a function of a buffer width during 2009–2017.

water quality.

4. Conclusions

This study was carried out to understand the extent, frequency and nature of hydraulic and solute dynamics relationship between river and irrigated crops interspersed with a buffer. The calibrated and validated model (HYDRUS-2D) was used to evaluate long-term (8 years) scenarios involving different irrigated crops (wine grapes, almond, and annual horticulture) and varied buffer widths (10–110 cm) aimed at quantifying the hydraulic connection between the river and the crop grown and optimizing buffer width for controlling solute movement to the river.

Statistical evaluation (correlation coefficient, *ME, MAE, RMSE*, *t*-test and model efficiency) of the model for water movement showed a fairly good matching between the measured and the simulated water table depths. The results obtained from 8-years of simulations showed that three irrigated crops (wine grapes, almond, and annual horticulture) requiring different annual irrigation applications have markedly different influence on the overall water and solute movement within the crop-buffer-river ecosystem. Consequently, the average annual flow from the soil to the river was 2.1 and 1.8 times higher under almond and annual horticulture, respectively, compared to wine grapes. For average annual water balance to reach equilibrium, buffer (*Eucalyptus* spp.) widths of 20, 65, and 55 m were needed for wine grapes, almond, and annual horticultural crops (carrot-potato), respectively.

From the standpoint of migration of irrigation induced soluble salts into the river, the buffer widths of 20, 60, and 40 m were able to reduce the salt load by > 99% under wine grapes, almond, and annual horticulture crops, respectively. Notably, existing guidelines do not differentiate between crop types when specifying optimum buffer widths. Further work is required to assess how the seasonal variability in irrigation water quality influences these results, particularly in areas where recycled water is used for irrigation. The modelling challenges and data limitations included the absence of preferential flow, the assumption of similar water stress response functions for the buffer vegetation and irrigated crops, and lack of data for calibration of the model against solute dynamics in the river. Further refinements in the above findings may be achieved by addressing these gaps.

Declaration of interests

None declared.

Acknowledgments

Authors highly acknowledge the financial support by the Goyder Institute for Water Research for this work under the project “Sustainable Expansion of irrigated Agriculture and Horticulture in Northern Adelaide Corridor (Project Number ED-17-01).”

References

Alaghmand, S., Beecham, S., Hassanli, A., 2013. Impacts of groundwater extraction on salinization risk in a semi-arid floodplain. Nat. Hazards Earth Syst. Sci. 13, 3405–3418.

Alaghmand, S., Beecham, S., Hassanli, A., 2014. Impacts of vegetation cover on surface-groundwater flows and solute interactions in a semi-arid saline floodplain: a case study of the Lower Murray River. Australia. Environ. Process. 1, 59–71.

Allaire, S.E., Sylvain, C., Lange, S.F., Thériault, G., Lafrance, P., 2015. Potential efficiency of riparian vegetated buffer strips in intercepting soluble compounds in the presence of subsurface preferential flows. PLoS One 10 (7), 1–21. https://doi.org/10.1371/journal.pone.0131840. e0131840.

Allen, R.G., Pereira, L.S., Raes, D., Smith, M., 1998. Crop evapotranspiration guidelines for computing crop water requirements. FAO Irrigation and Drainage Paper No. 56, FAO, Rome, Italy.

ASRIS, 2011. Australian Soil Resource Information System. http://www.asris.com.au. Accessed on April 10, 2018.

Aubin, I., Beaudet, M., Messier, C., 2000. Light extinction coefficients specific to the understory vegetation of the southern boreal forest, Quebec. Can. J. For. Res. 30, 168–177.

Baker, T.T., Conner, W.H., Lockaby, B.G., Stanturf, J.A., Burke, M.K., 2001. Fine root productivity and dynamics on a forested floodplain in South Carolina. Soil Sci. Soc. Am. J. 65 (2), 545–556.

Baratelli, F., Flipo, N., Moatar, F., 2016. Estimation of stream-aquifer exchanges at regional scale using a distributed model: sensitivity to in-stream water level fluctuations, riverbed elevation and roughness. J. Hydrol. 542, 686–703.

Berens, V., White, M.G., Souter, N.J., 2009. Injection of fresh river water into a saline floodplain aquifer in an attempt to improve the condition of river red gum (*Eucalyptus camaldulensis* Dehnh.). Hydrol. Process. 23, 3464–3473.

Bryan, R.B., Hawke, R.M., Rockwell, D.L., 1998. The influence of subsurface moisture on hill system evolution. Earth Surf. Process. Landf. 23, 773–789.

Carr, K.J., Tongbi, T., Ercan, A., Levent Kavvas, M., 2018. Evaluating the applicability of a two-dimensional flow model of a highly heterogeneous domain to flow and environmental management. J. Am. Water Resour. Assoc. 24, 184–197.

Charles, S.P., Fu, G., 2015. Statistically Downscaled Projections for South Australia. Goyder Institute for Water Research, Technical Report No. 15/1, Adelaide, South Australia. http://www.goyderinstitute.org/_r91/media/system/attrib/file/82/CC%20Task%203%20CSIRO%20Final%20Report_web.pdf.

Coffey, M.E., Workman, S.R., Taraba, J.L., Fogle, A.W., 2004. Statistical procedures for evaluating daily and monthly hydrologic model predictions. Trans. ASAE 47, 59–68.

Cote, C.M., Bristow, K.L., Charlesworth, P.B., Cook, F.J., Thorburn, P.J., 2003. Analysis of soil wetting and solute transport in subsurface trickle irrigation. Irrig. Sci. 22, 143–156.

Department of Environment, Water and Natural Resources, 2016. Non-prescribed Surface Water Resources Assessment – Adelaide and Mount Lofty Ranges Natural Resources Management Region, DEWNR Technical report 2016/34. Department of Environment, Water and Natural Resources, Government of South Australia, Adelaide.

Deshi, K.E., Obasi, M.O., Odiaka, N.I., Kalu, B.A., Ifenkwe, O.P., 2015. Leaf area index values of potato (*Solanum tuberosum* L.) stored for different periods in different kinds of stores. IOSR J. Agric. Vet. Sci. 8, 9–19.

DeVito, K.J., Fitzgerald, D., Hill, A.R., Aravena, R., 2000. Nitrate dynamics in relation to lithology and hydrologic flow path in a river riparian zone. J. Environ. Qual. 29, 1075–1084.

FAO, 2011. The State of the World’s Land and Water Resources for Food and Agriculture (SOLAW) – Managing Systems at Risk. Food and Agriculture Organization of the United Nations, Rome and Earthscan, London http://www.fao.org/docrep/017/i1688e/i1688e.pdf.

FAO, 2016. AQUASTAT website. Food and Agriculture Organisation of the United Nations (FAO). http://www.fao.org/nr/water/aquastat/didyouknow/index3.stm. Accessed on 24th April 2018.

Feddes, R.A., Kowalik, P.J., Zaradny, H., 1978. Simulation of Field Water Use and Crop Yield. Simulation Monographs, Pudoc, Wageningen, The Netherlands.

Flipo, N., Mouhri, A., Labarthe, B., Biancamaria, S., Rivière, A., Weill, P., 2014. Continental hydrosystem modelling: the concept of nested stream–aquifer interfaces Hydrol. Earth Syst. Sci. 18, 3121–3149.

Ghazavi, R., Vali, A.B., Eslamian, S., 2012. Impact of flood spreading on groundwater level variation and groundwater quality in an arid environment. Water Resour. Manage. 26 (6), 1651–1663.

Green, G.P., 2010. Point and Regional Scale Modelling of Vadose Zone Water and Salt Fluxes in an Area of Intensive Horticulture. Thesis submitted to Flinders University, South Australia. https://flex.flinders.edu.au/file/27320d77-7088-4d13-8bc5-9c2b1fc4a071/1/Thesis-Green-2010.pdf.

Hansen, B., Reich, P., Sam Lake, P., Cavagnaro, T., 2010. Minimum Width Requirements for Riparian Zones to Protect Flowing Waters and to Conserve Biodiversity: A Review and Recommendations, Report to the Office of Water. Department of Sustainability and Environment, Victoria.

Hill, A.R., Vidon, P.G.F., Langat, J., 2004. Denitrification potential in relation to lithology in five headwater riparian zones. J. Environ. Qual. 33, 911–919.

Holzworth, D.P., Huth, N.I., deVoil, P.G., Zurcher, E.J., Herrmann, N.I., McLean, G., Chenu, K., van Oosterom, E.J., Snow, V., Murphy, C., Moore, A.D., Brown, H., Whish, J.P.M., Verrall, S., Fainges, J., Bell, L.W., Peake, A.S., Poulton, P.L., Keating, B.A., 2014. APSIM-evolution towards a new generation of agricultural systems simulation. Environ. Model. Softw. 62, 327–350. https://doi.org/10.1016/j.envsoft.2014.07.009.

Kidmose, J., Dahl, M., Engesgaard, P., Nilsson, B., Christensen, B.S.B., Andersen, S., Hoffmann, C.C., 2010. Experimental and numerical study of the relation between flow paths and fate of a pesticide in a riparian wetland. J. Hydrol. 386, 67–79.

King, S.E., Osmond, D.L., Smith, J., Burchell, M.R., Dukes, M., Evans, R.O., Knies, S., Kunickis, S., 2016. Effects of riparian buffer vegetation and width: a 12-year longitudinal study. J. Environ. Qual. 45, 1243–1251.

Klatt, S., Kraus, D., Kraft, P., Breuer, L., Wlotzka, M., Heuveline, V., Haas, E., Kiese, R., Butterbach-Bahl, K., 2017. Exploring impacts of vegetated buffer strips on nitrogen cycling using a spatially explicit hydro-biogeochemical modeling approach. Environ. Model. Softw. 90, 55–67.

Legates, D.R., McCabe, G.J., 1999. Evaluating the use of goodness-of-fit measures in hydrologic and hydroclimatic model validation. Water Resour. Res. 35, 233–241.

Mayer, P.M., Reynolds, S.K., McCutchen, M.D., Canfield, T.J., 2007. Meta-analysis of nitrogen removal in riparian buffers. J. Environ. Qual. 36, 1172–1180.

Moriasi, D.N., Arnold, J.G., Van Liew, M.W., Bingner, R.L., Harmel, R.D., Veith, T.L., 2007. Model evaluation guidelines for systematic quantification of accuracy in watershed simulations. Trans. ASABE 50, 885–900.

McKergow, L.A., Weaver, D.M., Prosser, I.P., Grayson, R.B., Reed, A.E., 2003. Before and after riparian management: sediment and nutrient exports from a small agricultural

catchment, Western Australia. J. Hydrol. 270 (3), 253–272.
Naiman, R.J., Décamps, H., Mcclain, M.E., 2005. Riparia, Ecology, Conservation, and Management of Streamside Communities. Elsevier Academic Press, Burlington, MA.
Nash, J.E., Sutcliffe, J.V., 1970. River flow forecasting through conceptual models, part I - A discussion of principles. J. Hydrol. 10, 282–290.
Overton, I., Jolly, I., 2004. Integrated studies of floodplain vegetation health, saline groundwater and flooding on the Chowilla floodplain, South Australia. CSIRO Land and Water Technical Report 20/04. http://www.clw.csiro.au/publications/technical2004/tr20-04.pdf.
Phogat, V., Cox, J.W., Šimůnek, J., 2018a. Identifying the future water and salinity risks to irrigated viticulture in the Murray-Darling Basin, South Australia. Agric. Water Manage. 201, 107–117.
Phogat, V., Pitt, T., Cox, J.W., Šimůnek, J., Skewes, M.A., 2018b. Soil water and salinity dynamics under sprinkler irrigated almond exposed to a varied salinity stress at different growth stages. Agric. Water Manage. 201, 70–82.
Phogat, V., Potter, N.J., Cox, J.W., Šimůnek, J., 2017a. Long-term quantification of stream-aquifer exchange in a variably saturated heterogeneous environment. Water Resour. Manage. 31, 4353–4366.
Phogat, V., Skewes, M.A., Cox, J.W., Sanderson, J., Alam, J., Šimůnek, J., 2014. Seasonal simulation of water, salinity and nitrate dynamics under drip irrigated mandarin (*Citrus reticulata*) and assessing management options for drainage and nitrate leaching. J. Hydrol. 513, 504–516.
Phogat, V., Skewes, M.A., Cox, J.W., Šimůnek, J., 2016. Statistical assessment of a numerical model simulating agro hydro-chemical processes in soil under drip fertigated mandarin tree. Irrigat. Drainage Sys. Eng. 5 (1), 1–9. https://doi.org/10.4172/2168-9768.1000155.
Phogat, V., Skewes, M.A., McCarthy, M.G., Cox, J.W., Šimůnek, J., Petrie, P.R., 2017b. Evaluation of crop coefficients, water productivity, and water balance components for wine grapes irrigated at different deficit levels by a sub-surface drip. Agric. Water Manage. 180, 22–34.
Ramos, T.B., Šimůnek, J., Goncalves, M.C., Martins, J.C., Prazeres, A., Castanheira, N.L., Pereira, L.S., 2011. Field evaluation of a multi-component solute transport model in soils irrigated with saline waters. J. Hydrol. 407, 129–144.
Rassam, D.W., 2011. A conceptual framework for incorporating surface–groundwater interactions into a river operation–planning model. Environ. Model. Softw. 26 (12), 1554–1567.
Reid, J.B., English, J.M., 2000. Potential yield in carrots (*Daucus carota* L.): theory, test, and an application. Ann. Bot. 85, 593–605.
Reynolds, A.G., 2010. Viticultural and vineyard management practices and their effects on grape and wine quality. In: Reynolds, A.G. (Ed.), Managing wine Quality Volume 1: Viticulture and Wine Quality. Woodhead Publishing, Cambridge, pp. 365–444.
Ritchie, J.T., 1972. Model for predicting evaporation from a row crop with incomplete cover. Water. Resour. Res. 8, 1204–1213.
Rousseau, A.N., Lafrance, P., Lavigne, M., Savary, S., Konan, B., Quilbé, R., Jiapizian, P., Amrani, M., 2012. A hydrological modeling framework for defining achievable performance standards for pesticides. J. Environ. Qual. 41, 52–63.
Schilling, K.E., Jacobson, P.J., Wolter, C.F., 2018. Using riparian Zone scaling to optimize buffer placement and effectiveness. Landscape Ecol. 33, 141–156.
Šimůnek, J., van Genuchten, M.Th., Šejna, M., 2016. Recent developments and applications of the HYDRUS computer software packages. Vadose Zone J. 15 (7), 1–25. https://doi.org/10.2136/vzj2016.04.0033.
Sophocleous, M., 2010. Groundwater management practices, challenges, and innovations in the High Plains aquifer, USA – lessons and recommended actions. Hydrogeol. J. 18 (3), 559–575.
Stevens, D.P., McLaughlin, M.J., Smart, M.K., 2003. Effects of long-term irrigation with reclaimed water on soils of the Northern Adelaide Plains, South Australia. Aust. J. Soil Res. 41, 933–948.
Xian, Y., Jin, M., Liu, Y., Si, A., 2017. Impact of lateral flow on the transition from connected to disconnected stream–aquifer systems. J. Hydrol. 548, 353–367.
Xiao, Q., McPherson, E.G., Ustin, S.L., Grismer, M.E., Simpson, J.R., 2000. Winter rainfall interception by two mature open-grown trees in Davis, California. Hydrol. Process. 14, 763–784.
Zhang, X., Liu, X., Zhang, M., Dahlgren, R.A., Eitzel, M., 2010. Vegetated buffers and a meta-analysis of their mitigation efficacy in reducing non-point source pollution. J. Environ. Qual. 39, 76–84.